CHAPTER IV

RESULTS AND DISCUSSION

In this research, alumina nanofibers were synthesized by calcination of boehmite/polymer composite nanofibers that were obtained from combining the sol-gel process with the electrospinning technique. Effects of many factors involving in the synthesis process were investigated and will be described in this chapter. The chapter can be divided into 4 sections as followed:

Section 4.1 presents the results from the preliminary experiments of alumina nanofibers synthesis.

Section 4.2 describes effects of morphology (i.e. powder or nanofibers) on phase transformation and crystallite structure of alumina.

Section 4.3 describes effects of hydrolysis time on viscosity of electrospinning solution as well as size distribution of as-spun fibers.

Section 4.4 describes effects of pH of the electrospinning solution on the structure of alumina nanofibers.

4.1 PRELIMINARY EXPERIMENTS

In the preliminary experiments, alumina powders were prepared by sol-gel technique using of aluminum isopropoxide (AIP) as precursor. After heating a mixture of AIP and water at 80°C under constant stirring for 1 h, the mixture became slurry. Then, acetic acid was added to this slurry as a peptizing agent. Typically, molar ratio of water, AIP and acetic acid was 100:1:0.15 [Kobayashi et al. 2005]. The powder was obtained after drying the solution in an oven at 110°C overnight and subsequently calcining at 1,200°C for 2 hrs. It was found from XRD analysis that the powder before and after calcination was boehmite and α-Al_2O_3, respectively (see Figure 4.1 and 4.2)
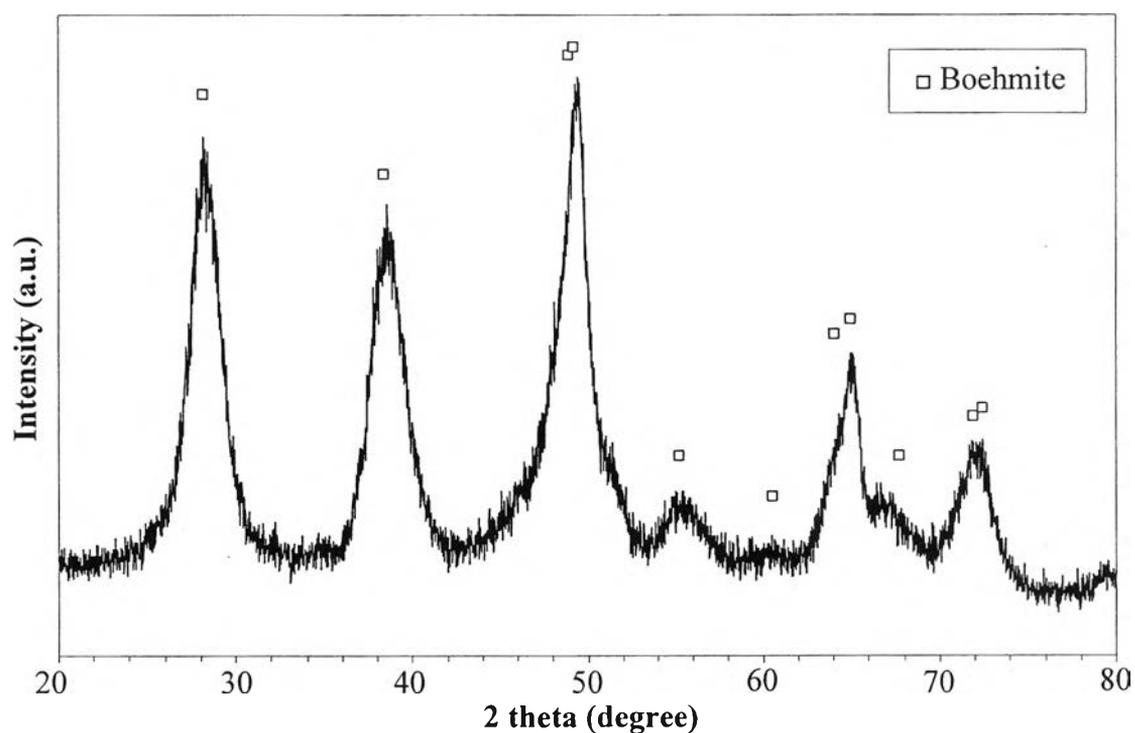
Figure 4.1 XRD pattern of dried powder obtained from sol-gel process, before calcination.
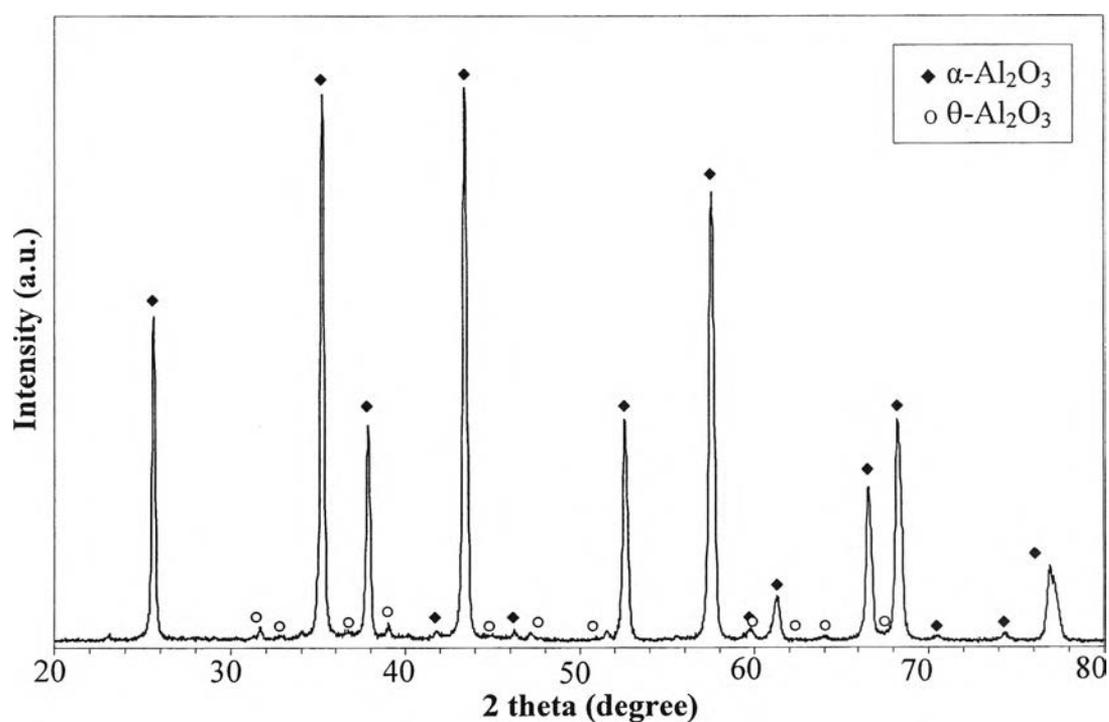
Figure 4.2 XRD pattern of powder obtained from sol-gel process and subsequently calcined at 1,200°C for 2 hrs.

The presence of crystalline entities within the dried powder obtained from the sol-gel process, which is confirmed by XRD analysis to be boehmite, can also be observed from TEM micrograph in Figure 4.3. At high magnification (Figure 4.3(b)), lattice fringes are clearly seen. Figure 4.3 also shows that the synthesized powder is in fact consisted of many nanoparticles. Size of these particles is less than 5 nm, which conform to the value calculated by the Scherer's equation. The clear lattice fringes and the sharps potted pattern in the selected area electron diffraction pattern (SAED) (Figure 4.3(c)) indicate that the particle is indeed single crystal.

(a)

(b)

(c)
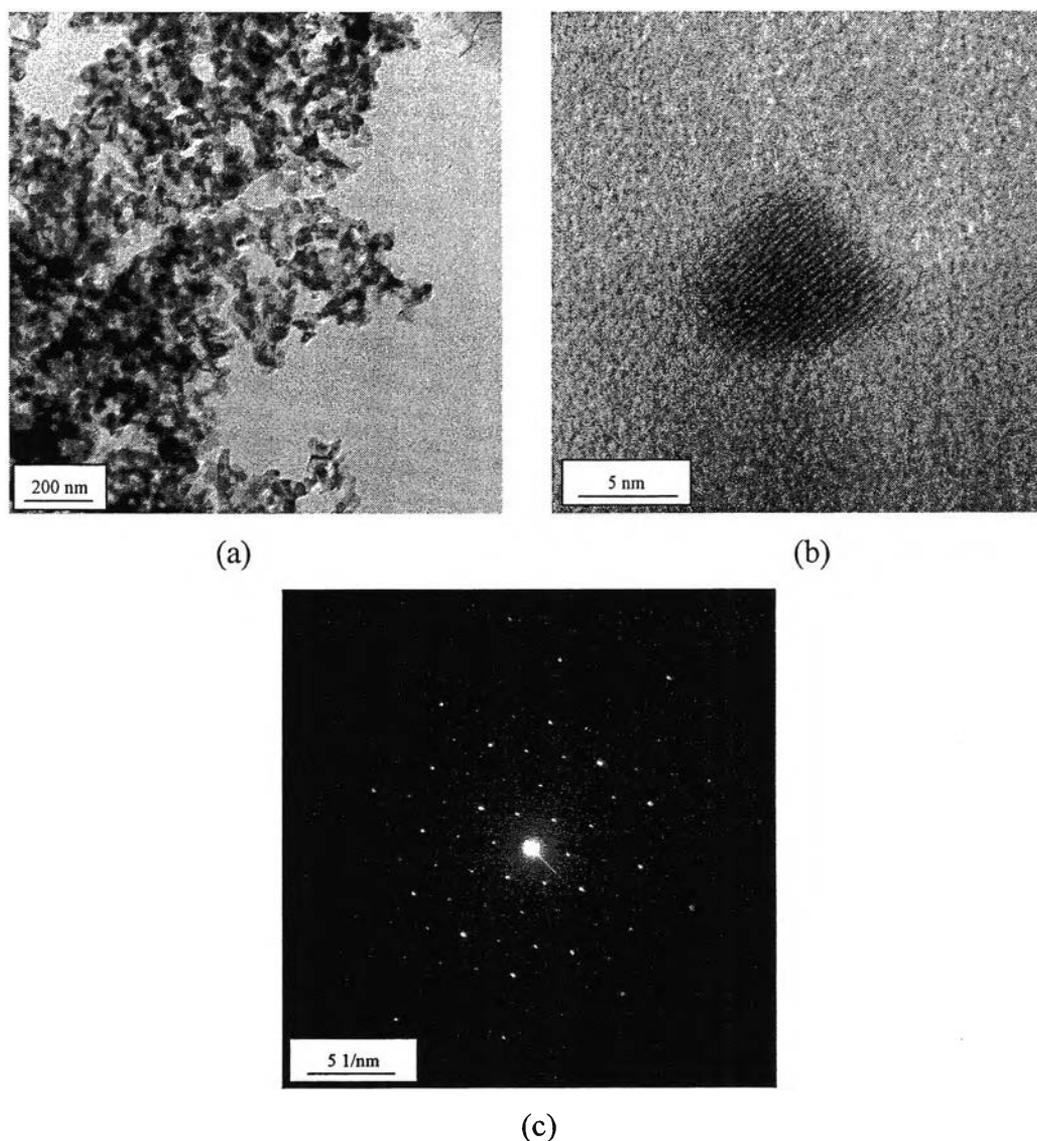
Figure 4.3 TEM micrographs of dried powder obtained from sol-gel process: (a) low-magnification TEM image (b) high resolution TEM image and (c) SAED pattern.

For the synthesis of alumina nanofibers via the combined sol-gel and electrospinning process, the electrospinning solution was composed of AIP as precursor, poly vinylalcohol (PVA; M_w of 73,000) as spinning aid, acetic acid as peptizing agent and water as solvent. By applying electric field strength of 8.5 kV across the syringe needle and the collector plate, which were set at 12 cm apart, ultrafme fibers were spun and deposited as a non-woven mat on the collector plate.

XRD pattern of as-spun fibers is shown in Figure 4.4(a). According to this graph, the as-spun fibers are mainly amorphous due to the nature of the polymer which is the main constituent in the fiber. Nevertheless, according to the preliminary results of dried sol (Figure 4.1), it is suggested that the as-spun fibers are boehmite/PVA fibers, but the fraction of boehmite is too low to reflect strong XRD signal. The fibers are transformed to crystalline α-Al_2O_3 during the calcination as shown in Figure 4.4(b).
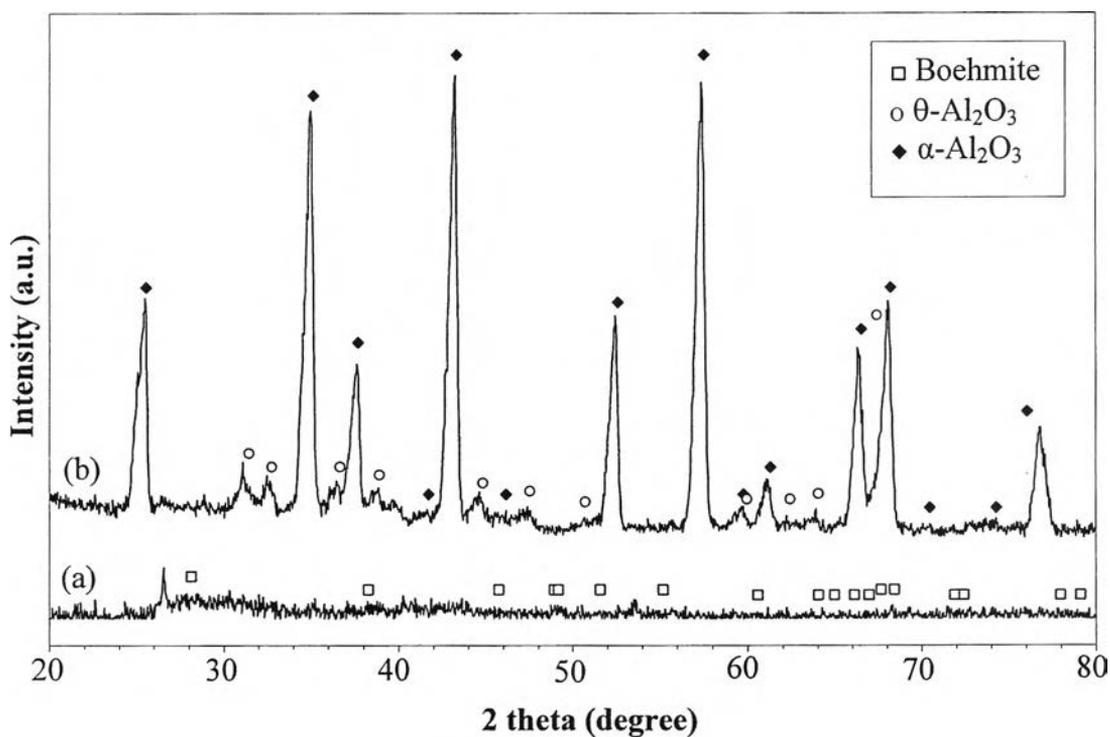
Figure 4.4 XRD patterns of: (a) as-spun fibers obtained from electrospinning process and (b) fibers calcined at 1,200°C for 2 hrs.

In this study, PVA in the as-spun composite fibers was removed by controlled calcination, leaving only alumina in calcined fibers. Although this result will be discussed in more detail in the next section, it was preliminarily confirmed by the result from TGA-DTA analysis in oxygen atmosphere as shown in Figure 4.5 that PVA goes through complete combustion when the temperature reach to 500°C. It should be noted that Figure 4.5 shows the analysis results of the sample formed without electrospinning in order to avoid the coupling effect from morphology of the fiber.
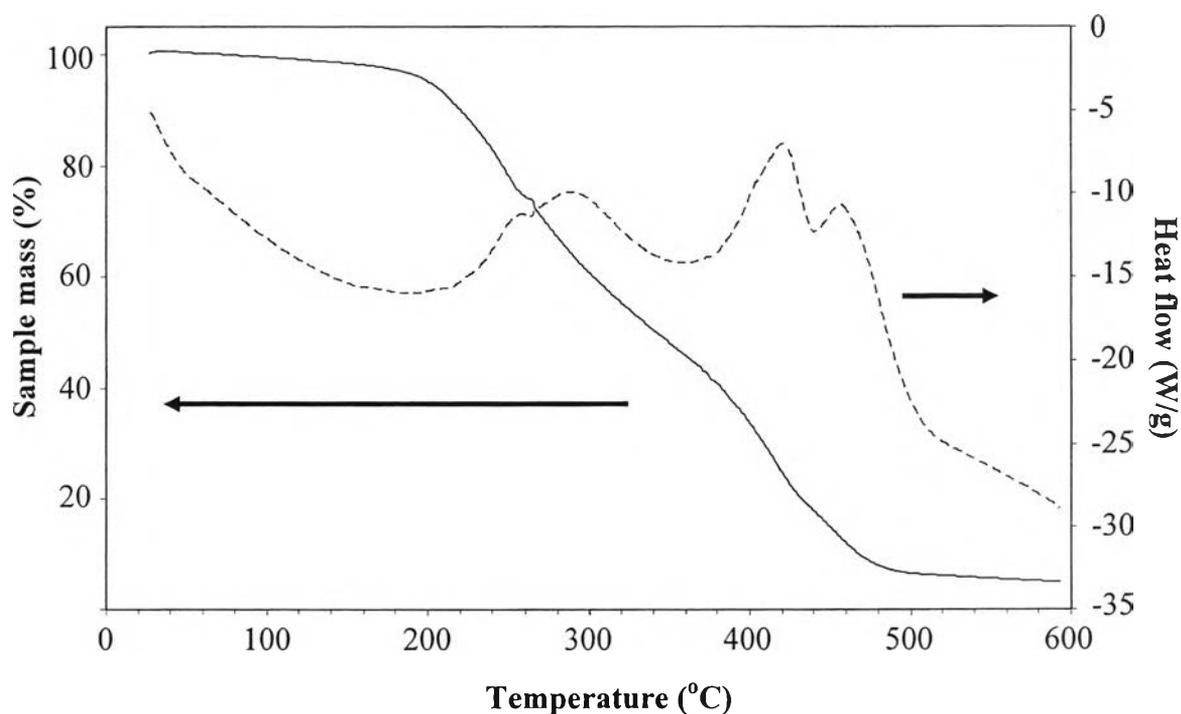
Figure 4.5 Thermogravimetric curves of the pure PVA analyzed in oxygen atmosphere.

Electron micrographs of the as-spun boehmite/PVA composite fibers and the calcined fibers are shown in Figure 4.6 and 4.7, respectively. It is found that the as-spun fibers generally have diameter in nanometer scale, in the range from 90 to 120 nm, but the fibers are very long. The surface of the as-spun fiber is smooth due to the amorphous nature of the boehmite/PVA composite. On the other hand, the physical property of fibers, inspected by visual observation, changes from flexible to brittle after the calcination. Although the SEM micrographs confirm that the calcined products are still in the form of fibers, morphology of the fibers is different from the

as-spun fibers because of the removal of organic component from the fibers as well as the growth of alumina grains within the fibers. It is the result from the fact that sol-gel process results in uniformly mixed mixture and therefore the spinning aid (i.e. PVA) contacts with boehmite derived from sol-gel process homogeneously. The results from the preliminary experiments indicate that α-Al_2O_3 nanofibers could be synthesized by combining sol-gel and electrospinning techniques.

(a)   (b)
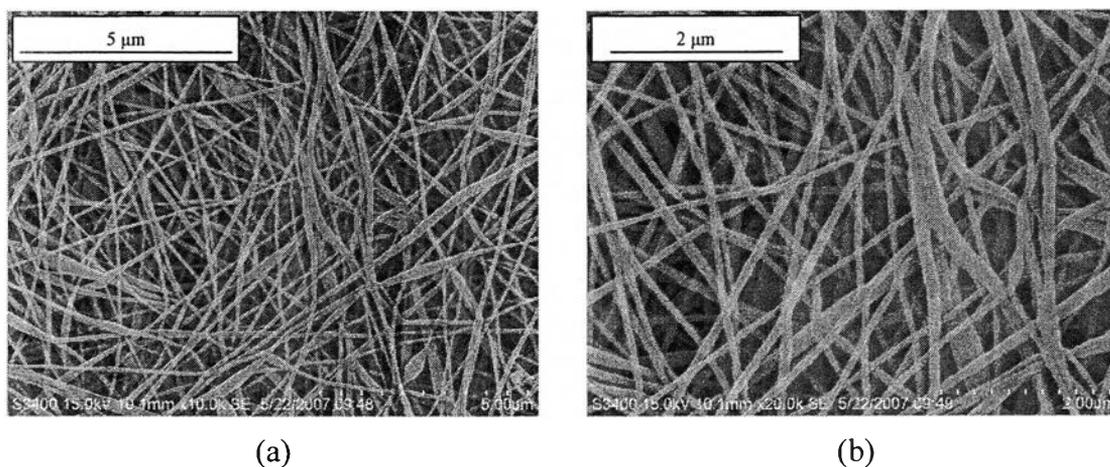
Figure 4.6 SEM images of the as-spun composite fiber: (a) low magnification and (b) high magnification.

(a)   (b)
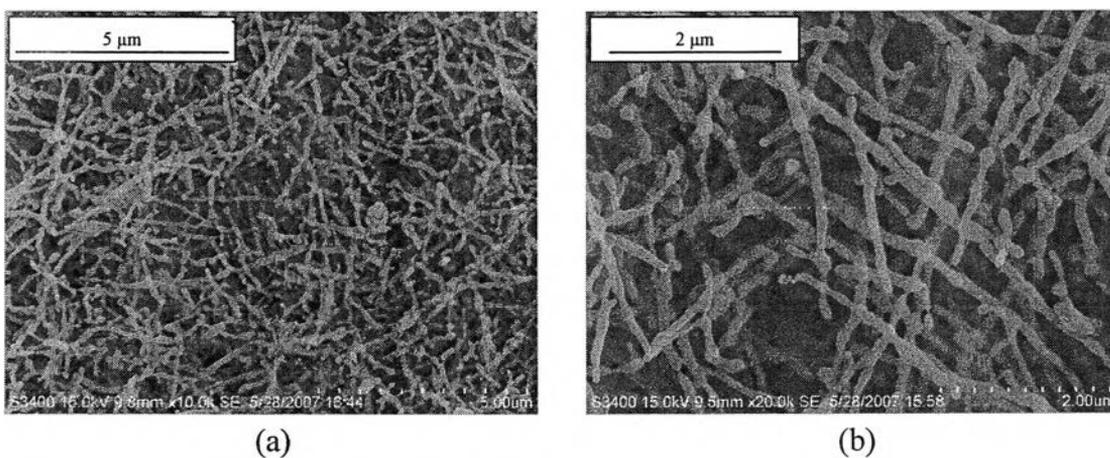
Figure 4.7 SEM images of the fibers calcined at 1,200°C for 2 hrs: (a) low magnification and (b) high magnification.

A TEM image in Figure 4.8(a) illustrates that the fibers, which were calcined at 1,200°C for 2 hrs, appear to be single crystals mixed with polycrystals. Morphology of the fiber is very similar to that observed earlier in the previous context (see Figure 4.7). Part of the fibers that seemed to be single crystal (e.g. as shown in Figure 4.8(b)) was further analyzed by SAED. The resulting pattern shown in Figure 4.8(c) clearly confirms the single-crystalline nature of the fiber.

(a)

(b)

(c)
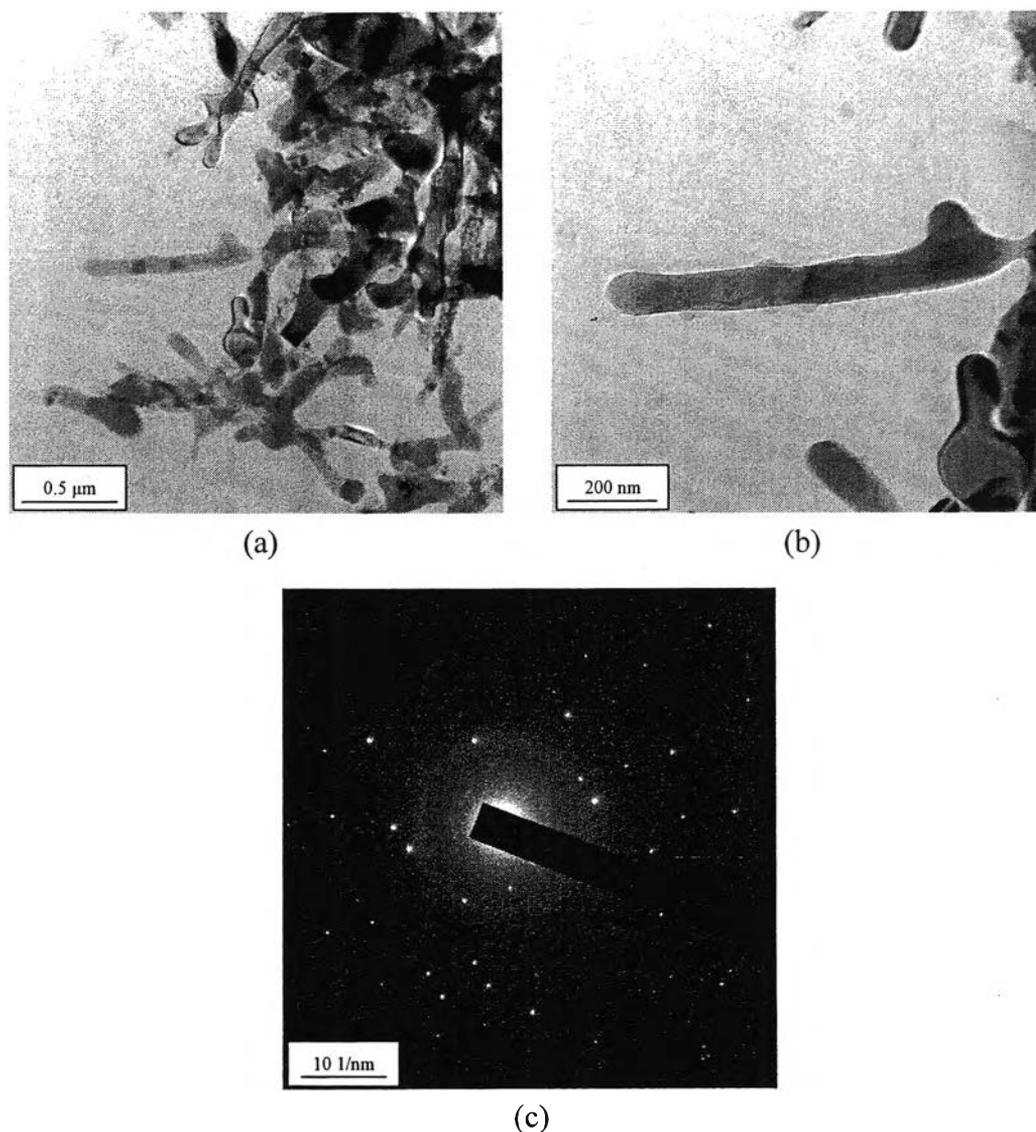
Figure 4.8 TEM micrographs of as-spun fibers calcined at 1,200°C for 2 hrs: (a) low magnification TEM image, (b) high magnification TEM image and (c) SAED pattern.

4.2 EFFECT OF MORPHOLOGY ON PHASE TRANSFORMATION

In this section, effect of morphology of product on phase transformation behavior, is investigated. Two types of product were used, i.e. boehmite powders obtained by drying of the product from sol-gel process, and boehmite/PVA composite fibers obtained from the electrospinning techniques. It should be noted that PVA was not mixed with the solution during the preparation of the boehmite powder. The solution was left in ambient atmosphere for one day for hydrolysis and removal of the solvent by natural evaporation. In the case of the fibers, the mixture from sol-gel process was mixed with 5.75 wt% PVA solution, as described in the previous chapter, prior to the electrospinning process. PVA was used to control the viscosity of the spinning solution. However, it was confirmed by the result from TGA-DTA analysis in oxygen atmosphere as shown in Figure 4.9, 4.10 and 4.11 that the presence of polymer does not affect the phase transformation from boehmite within the composite fibers to alumina. The phase transformation for both boehmite/PVA composite fibers and boehmite powders take place at approximately the same temperature and both complete at around 500°C.
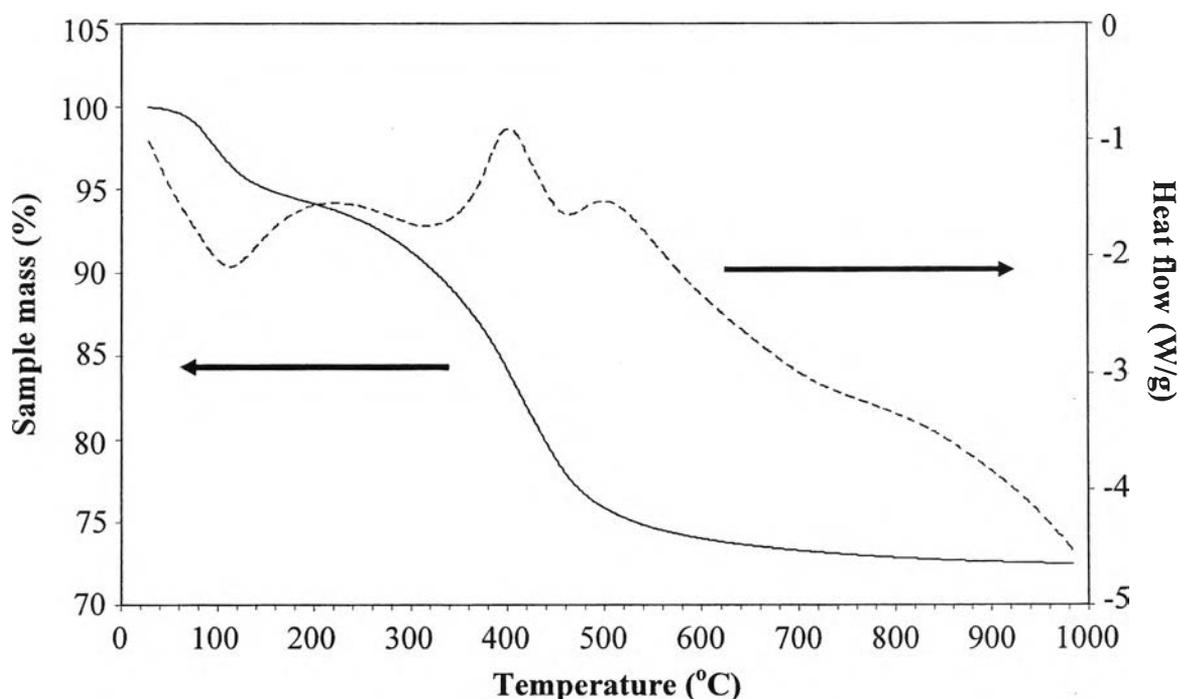
Figure 4.9 Thermogravimetric curves of the boehmite powder analyzed in oxygen atmosphere.
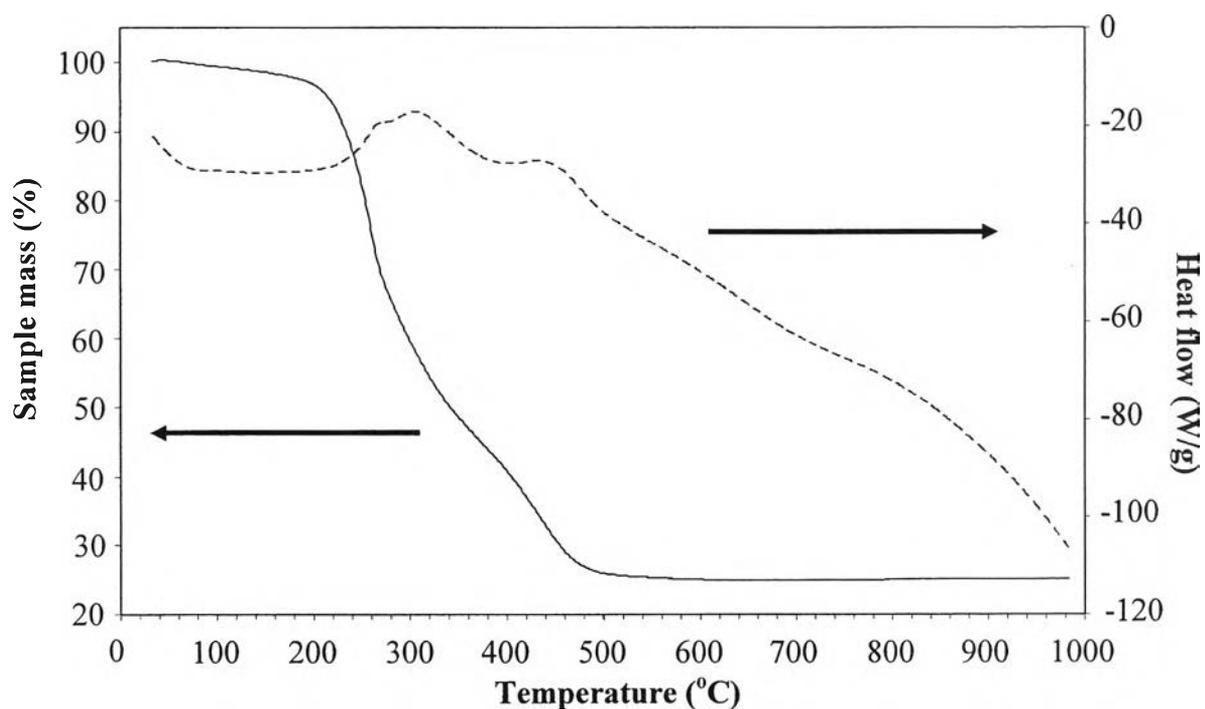
Figure 4.10 Thermogravimetric curves of the as-spun fibers analyzed in oxygen atmosphere.
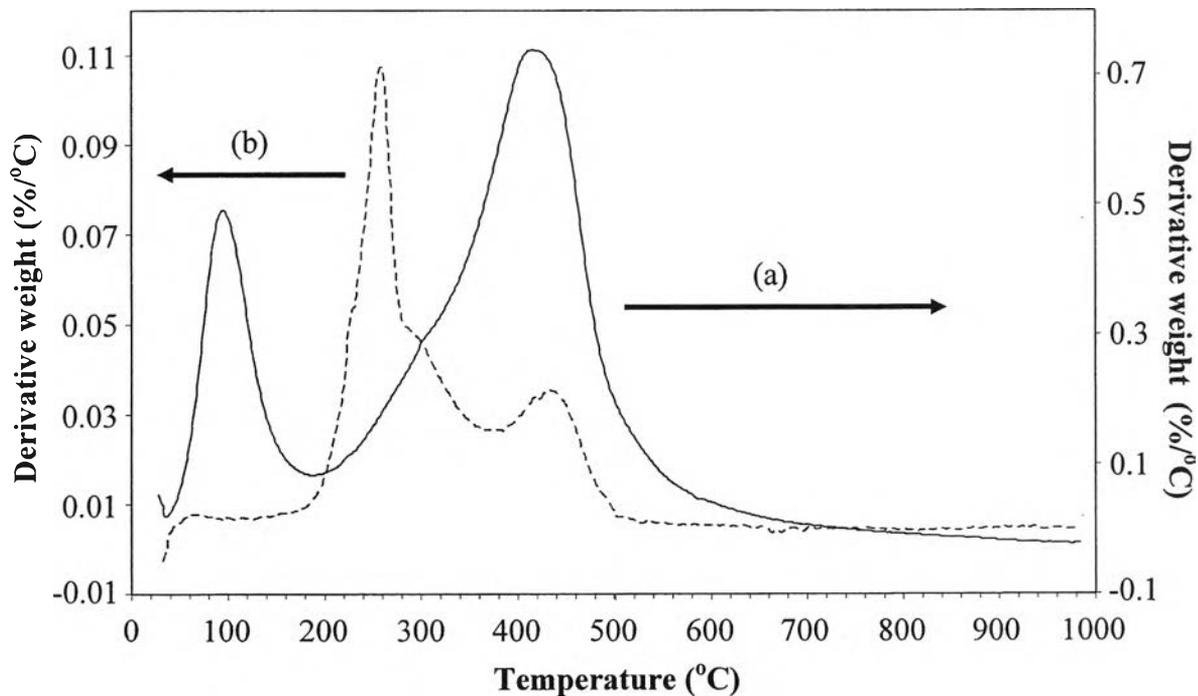
Figure 4.11 Derivatives of thermogravimetric curves for: (a) boehmite powders from sol-gel process and (b) as-spun fibers from electrospinning techniques.

It can be seen from Figure 4.9 that boehmite powder from sol-gel process shows weight loss about 20% at temperature between 150 to 500°C. Most of this loss takes place between 380 to 460°C. On the other hand, according to TGA-DTA curves in Figure 4.10, the as-spun fibers show total weight loss of about 70% at temperature between 180 to 500°C. However, the weight loss occurs in two steps. The first step of the weight loss about 50% occurs at temperature between 180 to 370°C, while another 20% of the weight loss occurs between 370 to 500°C. The first step of the weight loss occurs due to the loss of polymer within the fibers by combustion. The second one occurs accompanied with phase transformation from boehmite to γ-Al_2O_3 (detailed description on phase transformation will be discussed in the next paragraph). It should be noted that the weight loss around 100°C is considered as the result from the evaporation of water, which appears in both products. The derivatives of thermogravimetric curves in Figure 4.11 show that the transformation is completed at about 500°C. These results also indicate that thermal behaviors regarding phase transformation of boehmite powder and boehmite/PVA fibers are similar. There is no significant difference in phase transformation temperature for boehmite-to-γ-Al_2O_3 phase transformation from these two samples.

For detailed phase transformation investigation, the study was conducted by calcination of the products at various temperatures, in the range of 500 to 1,200°C, for 2 hrs and monitored crystalline phases via XRD analysis. Figure 4.12 shows pattern of boehmite powders transforming into crystalline alumina in α-phase by the calcination process. According to Figure 4.12, three steps of phase transition from boehmite to γ-Al_2O_3, θ-Al_2O_3 and finally to α-Al_2O_3 occur at temperature around 500, 900 and 1,100°C, respectively. The pattern of γ-Al_2O_3 can be clearly observed from the samples calcined between 500 and 800°C. For the sample calcined at 900°C, it starts to show a pattern of θ-Al_2O_3, which becomes more apparent as the calcination temperature is increased to 1,000°C. The diffraction patterns of the samples calcined at above 1,000°C clearly show characteristic peaks of α-Al_2O_3. However, θ-Al_2O_3 pattern can still be observed for the sample calcined at temperature as high as 1,200°C.
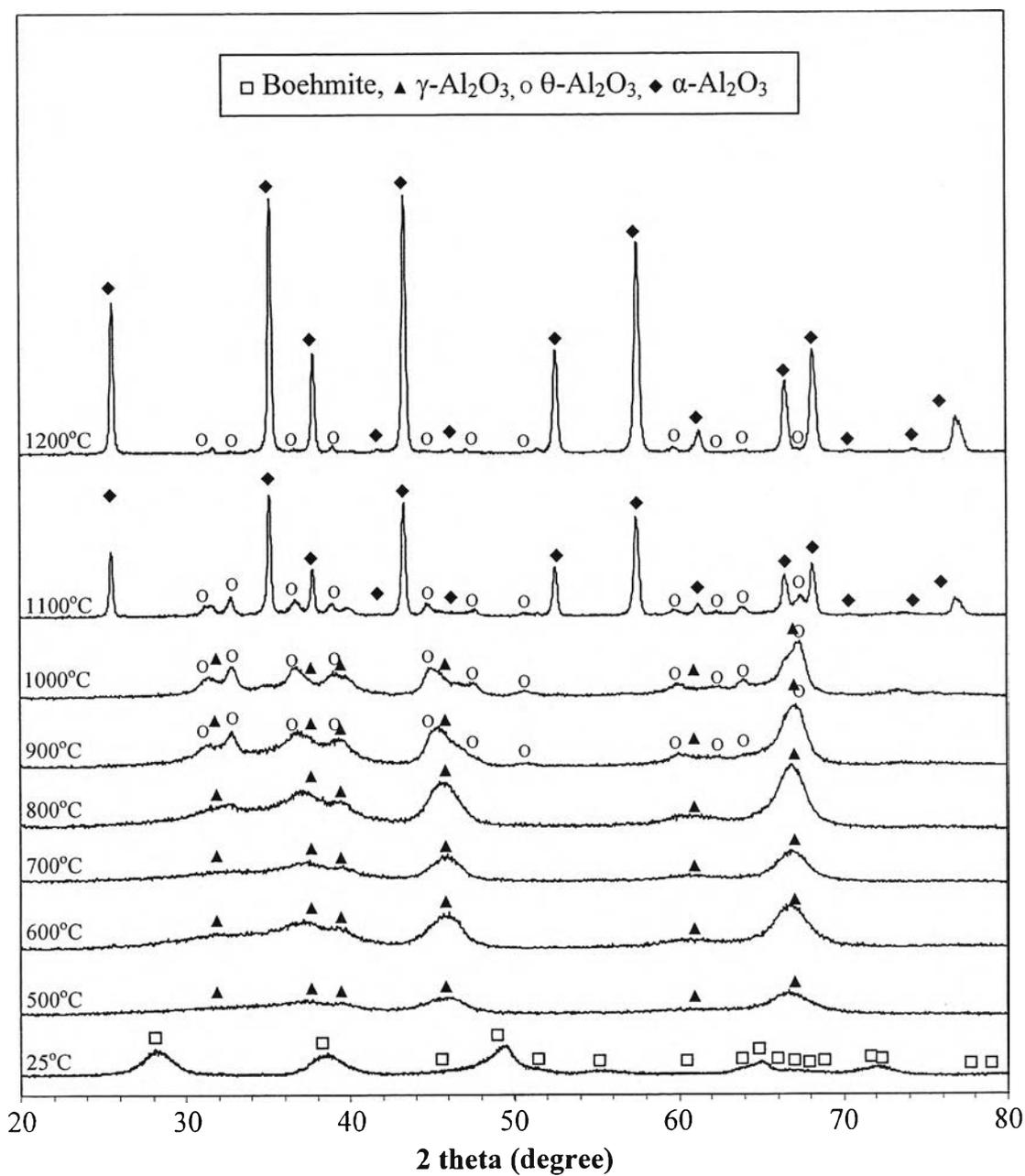
Figure 4.12 XRD patterns of boehmite powders calcined at various temperatures.

Similar variations in the diffraction patterns are also observed for electrospun fibers. Figure 4.13 shows XRD patterns of as-spun fibers calcined between 500 and 1,200°C. The γ-Al_2O_3 pattern is evident when the sample is calcined at 500°C and the sample is considered to be γ-Al_2O_3 until 800°C. The peaks representing θ-Al_2O_3 are initially observed at the calcination temperature around 900°C. Then, α-Al_2O_3 is formed and clearly identified at 1,100 and 1,200°C. Although the phase transformation sequences observed from the electrospun fibers are the same as those observed from the boehmite power, the pattern of as-spun fibers indicates amorphous nature instead of boehmite. This result is consistent with the results from TG-DTA and SEM, which referred to the existence of polymer as the major constituent in the as-spun fibbers.
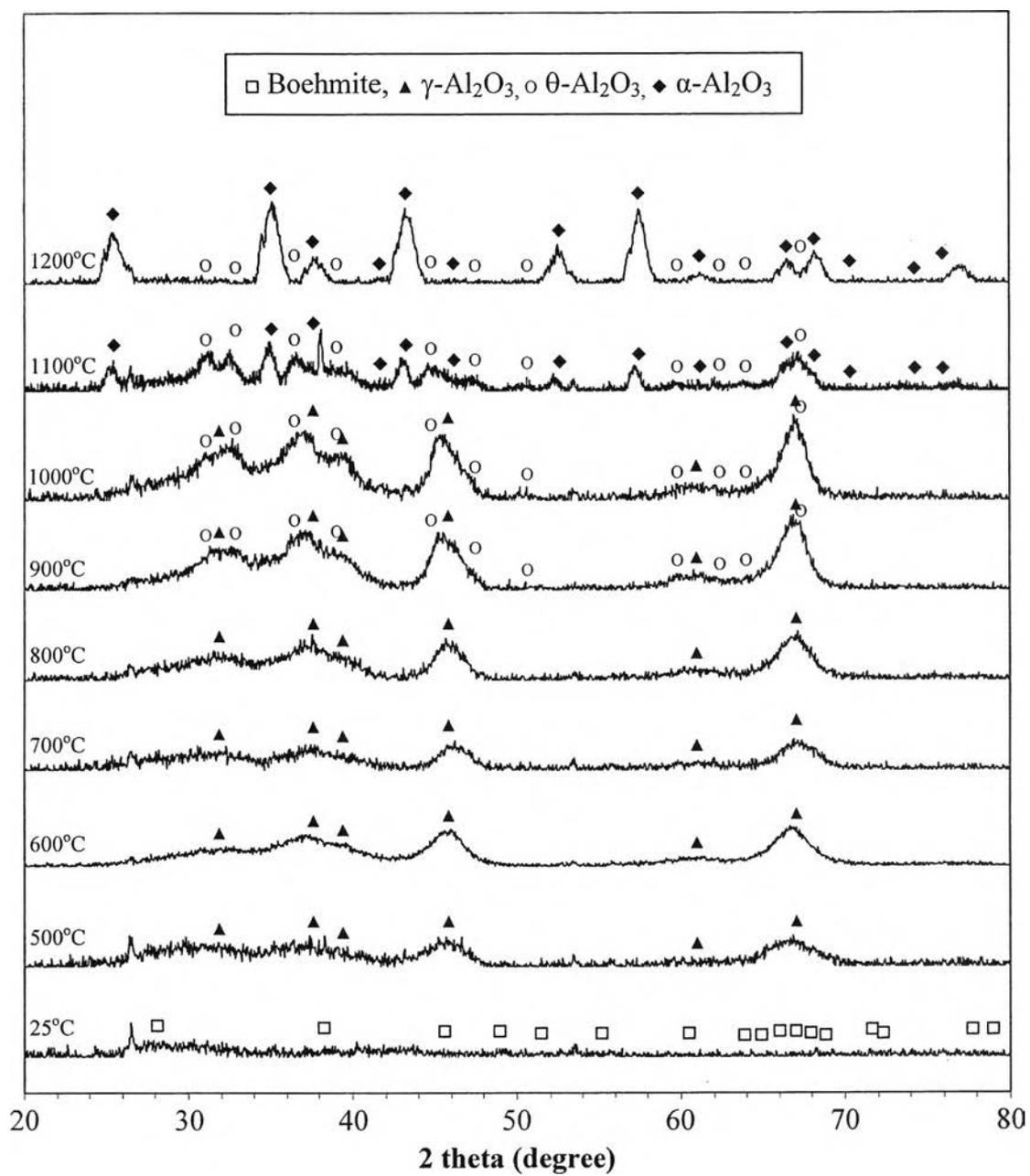
Figure 4.13 XRD patterns of electrospun fibers calcined at various temperatures.

In Figure 4.12 and 4.13, it is found that the crystallite size of alumina continues to grow as the thermal treatment proceeds, accompanied by phase transformation. The crystallite sizes of boehmite powder and electrospun boehmite/PVA composite fibers after calcined at various temperatures are summarized in Tables 4.1. The crystallite size was calculated by the Scherer's formula from the spread of XRD pattern. These results imply that calcination temperature is not the only factor affecting the average crystallite size of alumina in the product, but the morphology of the product as well. It is found that the crystallite size of calcined boehmite powder and calcined fibers are in the ranged from 3 to 16 and 3 to 90 nm, respectively. The difference in the crystallite size of θ-Al_2O_3 and α-Al_2O_3 is the result from the coalescence of the nuclei during phase transformation as well as the agglomeration of the crystallites during growth process. In powder form, θ-Al_2O_3 crystallites grow to size approaching 20 nm, before the nucleation of α-Al_2O_3 crystallite occurs. Subsequent growth of α-Al_2O_3 crystallites results in dramatic increase in crystallite size. It is found from Table 4.1 that the results in this work agree well with the results reported in literature [Wen and Yen 2008]. On the other hand, the crystallite size of α-Al_2O_3 in the electrospinning product is much smaller than that of the powder because the morphology as nanofibers restricts the growth to be one dimensional growth.

Table 4.1 Average crystallite size of alumina in products synthesized in powder and fiber form

T (°C)	Average crystallite size of alumina powders (nm)			Average crystallite size of alumina nanofibers (nm)		
	γ-Al_2O_3	θ-Al_2O_3	α-Al_2O_3	γ-Al_2O_3	θ-Al_2O_3	α-Al_2O_3
500	2.97			3.30		
600	3.98			3.54		
700	3.72			3.32		
800	4.15			4.10		
900		5.50			4.91	
1000		5.68			5.01	
1100		16.37	68.89		5.76	8.81
1200			89.15			15.83

The growth of crystallite size during phase transition from θ-to-α-Al_2O_3 is also supported by the results from TEM micrographs. Figure 4.14(a)-(c) show the TEM images of the as-spun fibers calcined at temperature of 1,000, 1,100 and 1,200°C, respectively. Grain boundary of the products calcined at 1,000 and 1,100°C cannot be clearly seen from TEM images, since the grains are heavily aggregated. Nevertheless, the TEM images reveal that grain size of the product calcined at 1,100°C is larger than that of the product calcined at 1,000°C. Moreover, it is found that the crystallite size of θ-Al_2O_3 within the fibers continues to grow as the thermal treatment proceeds, accompanied by the appearance of α-Al_2O_3 phase at temperature of 1,100°C, as summarized from XRD results (Figure 4.13). However, grain boundary between θ-Al_2O_3 and α-Al_2O_3 cannot be clearly observed. It should also be noted that although the product calcined at 1,200°C is mainly large grained fibers, some parts of the product are still fibers consisting of numbers of small aggregated grains.

(a)

(b)

(c)
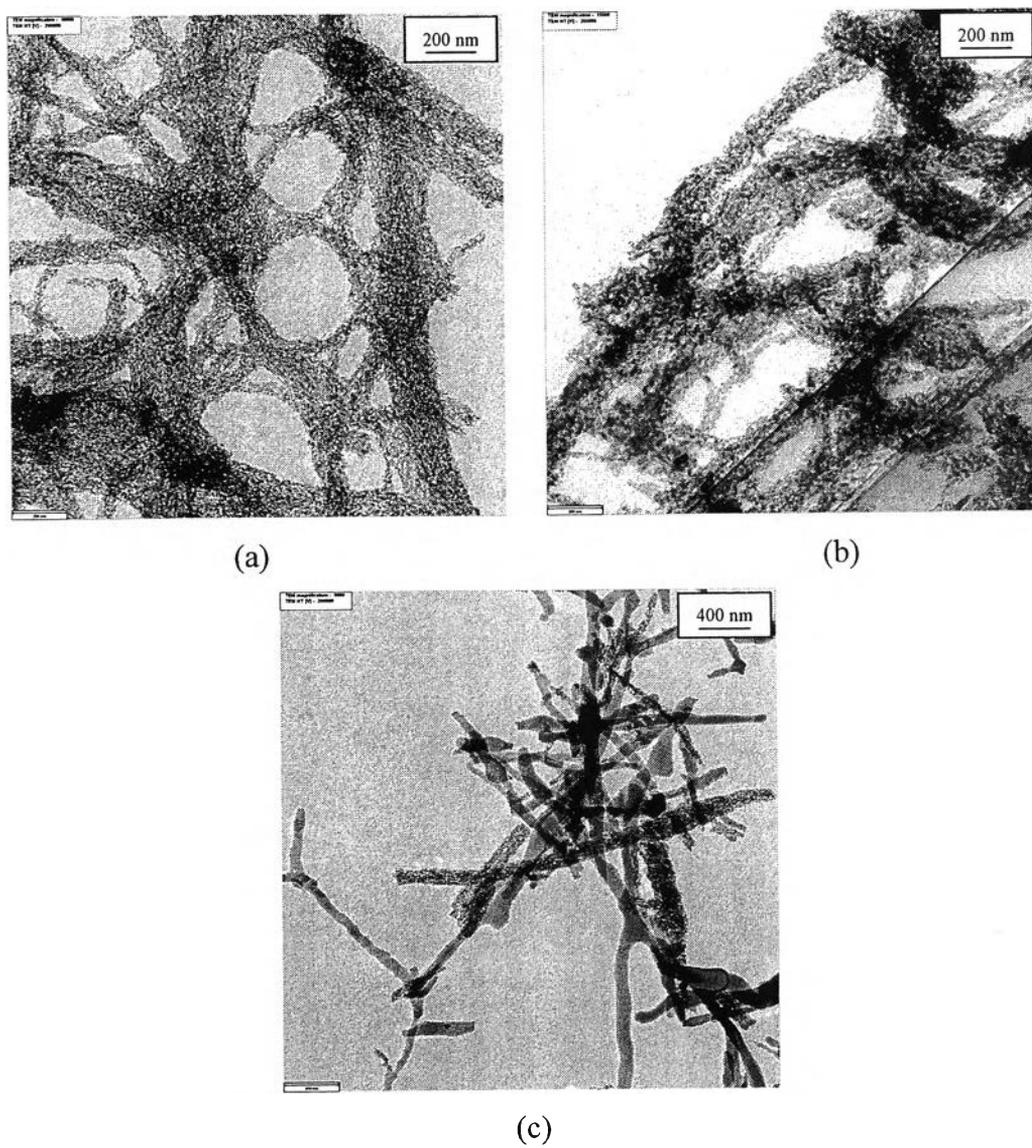
Figure 4.14 TEM micrographs of as-spun fibers calcined at 1,000°C (a), 1,100°C (b), and 1,200°C (c) for 2 hrs.

In Figure 4.15(a), fibers that are consisting of large-grain and aggregated-grains are compared, while Figure 4.15(b) and (c) show SAED images of the large-grain and aggregated-grains fiber. Unlike the aggregated small grains, size of the large grain observed in the TEM image is much larger than the crystallite size of 20 nm calculated from XRD broadening. Thus, it is suggested that the large grain observed is in fact polycrystals, even though grain boundaries were not clearly observed by TEM. On the other hand, aggregated-grains, which are referred to as secondary particle, are occurred by agglomeration of single crystalline particles. This remark is also supported by scattered SAED pattern in Figure 4.15(b), showing that the diffracted beams are originated from grains with different crystallographic orientations.
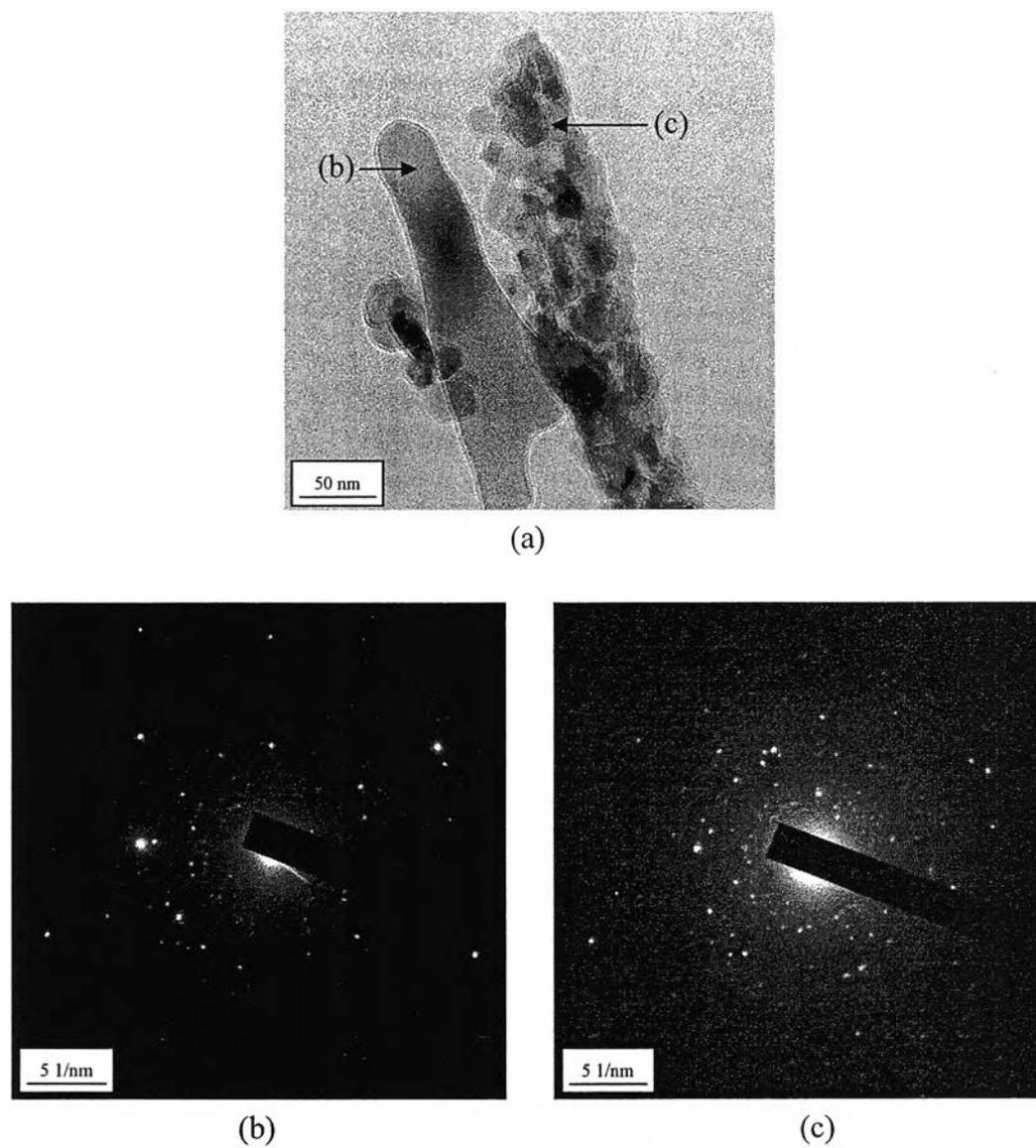
Figure 4.15 TEM micrographs of electrospun fibers calcined at 1,200°C for 2 hrs: (a) TEM image, (b) SAED pattern of fiber that is consisting of one large grain and, (c) SAED pattern of fiber that is consisting of number of small grains.

F 2443307X

4.3 EFFECTS OF AGING TIME

For the electrospinning process, the spinning solution must consist of polymer of sufficient molecular weight or concentration in order to achieve proper viscosity. One of the factors that affect viscosity of the solution is aging time. In order to investigate the effect of aging time, electrospinning solutions were prepared by using different periods of aging time, i.e. 8, 24 and 48 hrs. These values were chosen to obtain sufficient viscosity for forming fiber and to cover the gelling point of the solution. Figure 4.16 shows viscosity of the electrospinning solution with 5.75 wt% PVA, after it has been aged at 85°C for various periods of time. As the sol is concentrated, the colloidal particles movement transforms from a transitory to an oscillatory one [Yoldas 1975]. Thus, the viscosity of the solution increases as the aging time is increased. According to Figure 4.16, the viscosity of the system changes strikingly after 24 hrs of aging. When the viscosity of the electrospinning solution becomes too high, the solution may not flow through the nozzle property and it may dry up at the tip of the needle before the electrospinning can be initiated. Therefore, 24 hrs of aging was used as the point where the sol is viscous enough to prevent electrospray, yet not too viscous to inhibit electrospinning.
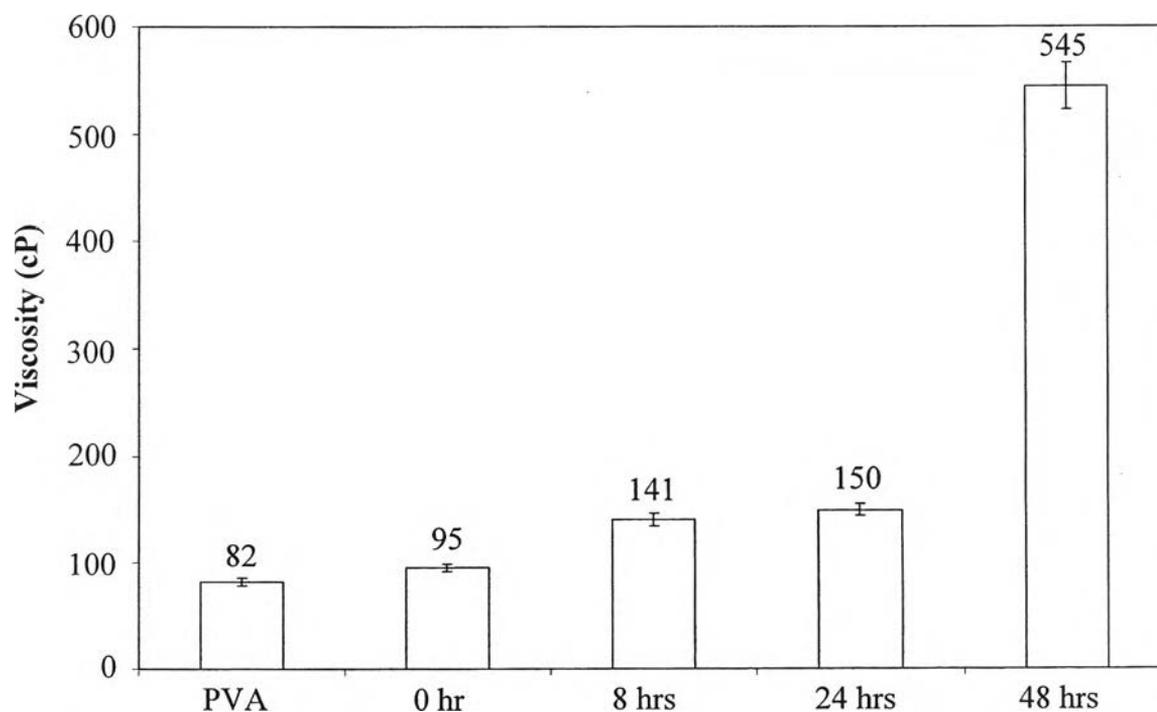
Figure 4.16 Viscosity of electrospinning solution with 5.75wt% PVA after aged for different periods of time.

The reactions that formed the polymeric network of inorganic materials during sol-gel process were described by Yoldas, which revealed that boehmite was formed as colloidal particles after hydrolysis and condensation reactions. Aging under heat treatment provided links among these particles into three dimensional structures [Yoldas 1975]. Thus, property of gel is significantly affected by aging temperature and time [Yoldas 1984]. This conclusion supports the results shown in Figure 4.16. The size distributions of the as-spun fibers were determined from SEM images as shown in Figure 4.17 and 4.18, using image analysis software (SemAfore). It can be seen that size of the fibers electrospun after aged for 8 hrs is less uniform than when the aging time of 24 hrs was employed. In this system, the effect from aging is more pronounced at high concentration of the polymeric network as reported by the study of Yoldas [Yoldas 1984]. This effect also reflects on the formation of nanofibers as shown in Figure 4.17. Beaded fibers are less likely to be formed from the solution prepared with prolonged aging time. As reported by Fong et al., the the shape of the beads changes from spherical to spindle-like [Fong et al. 1999]. Therefore, the disappearance of beds from the fibers electrospun after aged for 24 hrs (Figure 4.18) is the result from the increased viscosity of the spinning solution.
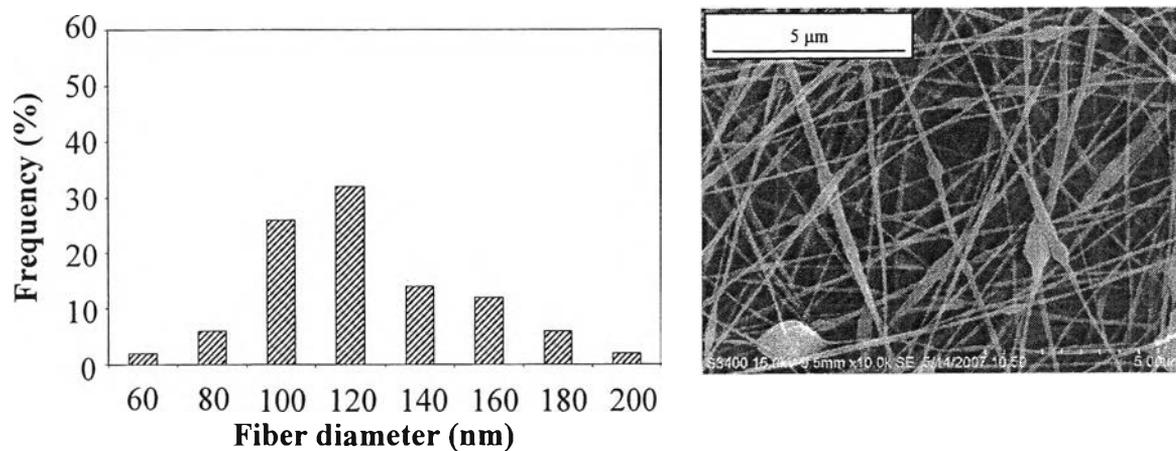
Figure 4.17 Size distribution and SEM image for fibers electrospun after aged for 8 hrs.
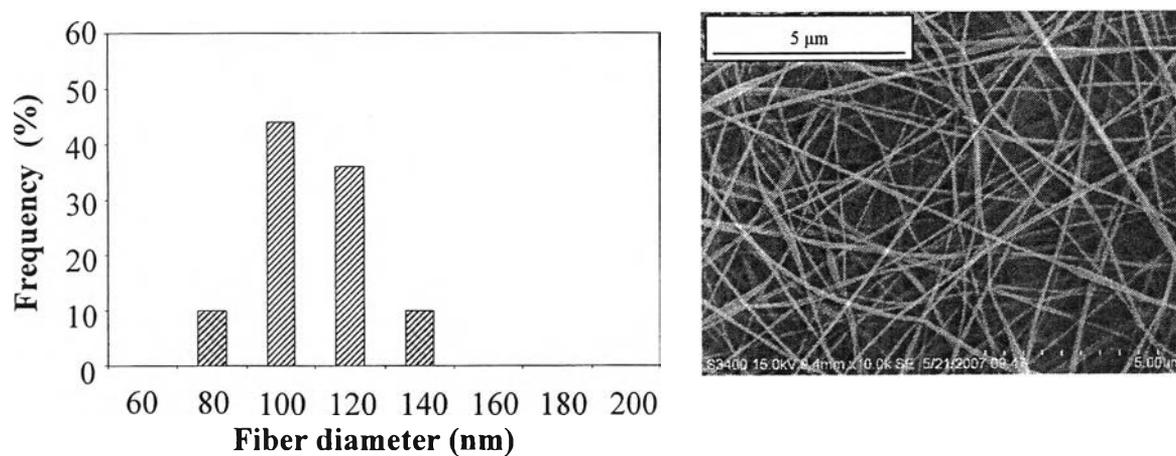
Figure 4.18 Size distribution and SEM image for fibers electrospun after aged for 24 hrs.

4.4 EFFECTS OF ACID DURING SOL-GEL PROCESS

The X-ray diffraction analysis results of dried powders prepared from the solution with significant different amount of acid, i.e. acid-to-AIP molar ratio of 0.15 and 1.5, are compared. Both show characteristic patterns of boehmite (Figure 4.19(a) and (b)), as previously described in Section 4.1. The difference between the experimental diffraction patterns and the theoretical values was also investigated. It can be seen from Figure 4.19(a) that the peak at 2θ around 49° shifts from the theoretical value by about 0.5°. This deviation becomes visibly reduced when the acid-to-AIP molar ratio is increased to 1.5 (Figure 4.19(b)). Therefore, the crystalline distortion is reduced by increased amount of acid in the prepared solution.
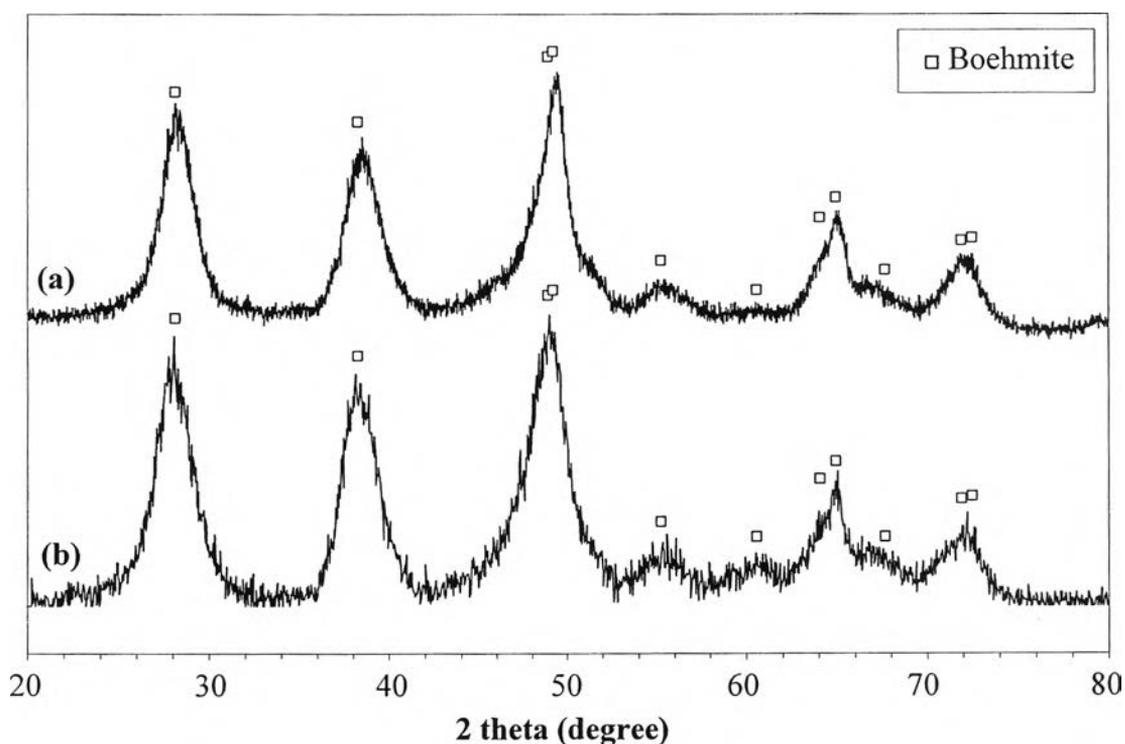
Figure 4.19 XRD patterns of dried boehmite powders prepared from the solution with acid-to-AIP molar ratio of: (a) 0.15:1 and (b) 1.5:1.

Figure 4.20 shows XRD patterns of the boehmite powders prepared by using the acid-to-AIP molar ratio of 0.15 and 1.5, after calcination at 1,100 and 1,200°C for 2 hrs. It confirms that all products are mainly α-Al₂O₃ after calcined at 1,200°C (Figure 4.20(a) and (c)). However, it should be noted that the fraction of θ-Al₂O₃ presented in the powder prepared by using the acid-to-AIP ratio of 1.5:1 is higher than the fraction in the sample prepared with lower acid ratio. The effect of acid is greatly evident in the samples calcined at 1,100°C, as shown in Figure 4.20(b) and (d). The sample prepared with the acid-to-AIP ratio of 0.15 is mainly α-Al₂O₃, with minor fraction of θ-Al₂O₃ observed. On the contrary, the major peaks of θ-Al₂O₃ are observed when the acid-to-AIP ratio is increased to 1.5. The phase transition is clearly retarded by high content of acid.
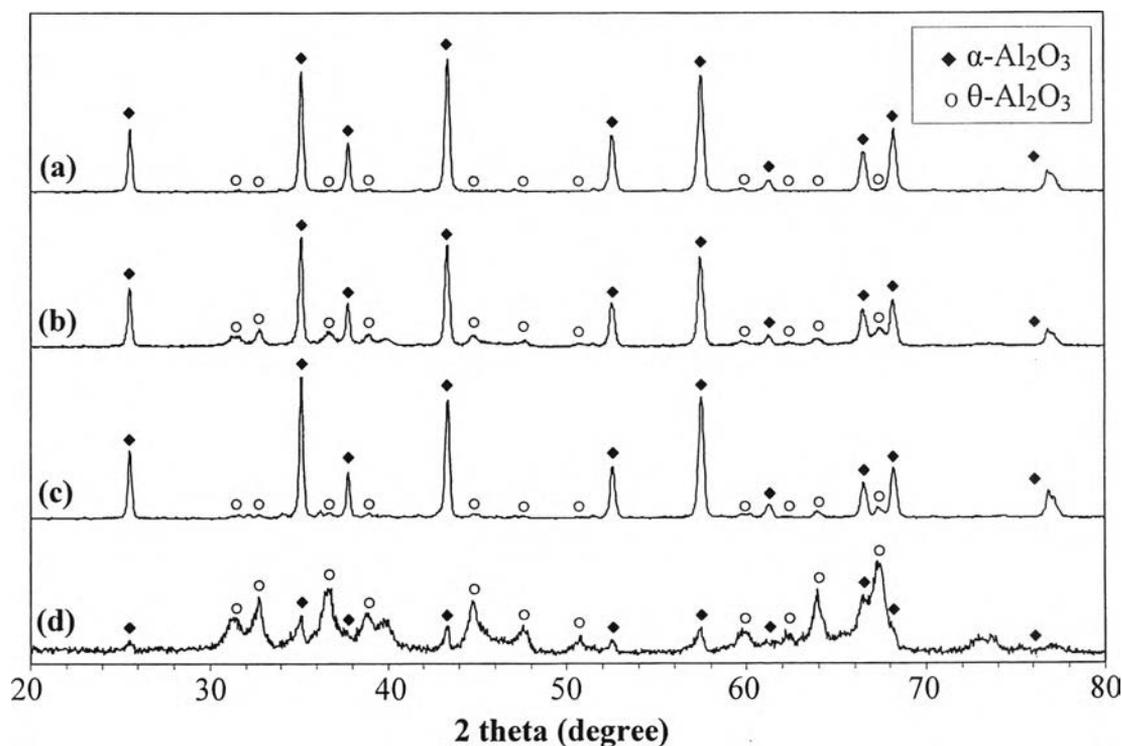
Figure 4.20 XRD patterns of boehmite powders prepared with acid-to-AIP molar ratio of 0.15:1, after calcined at 1,200°C (a) and 1,100°C (b) for 2 hrs and that of the powders prepared with acid-to-AIP molar ratio of 1.5:1, after calcined at 1,200°C (c) and 1,100°C (d) for 2 hrs.
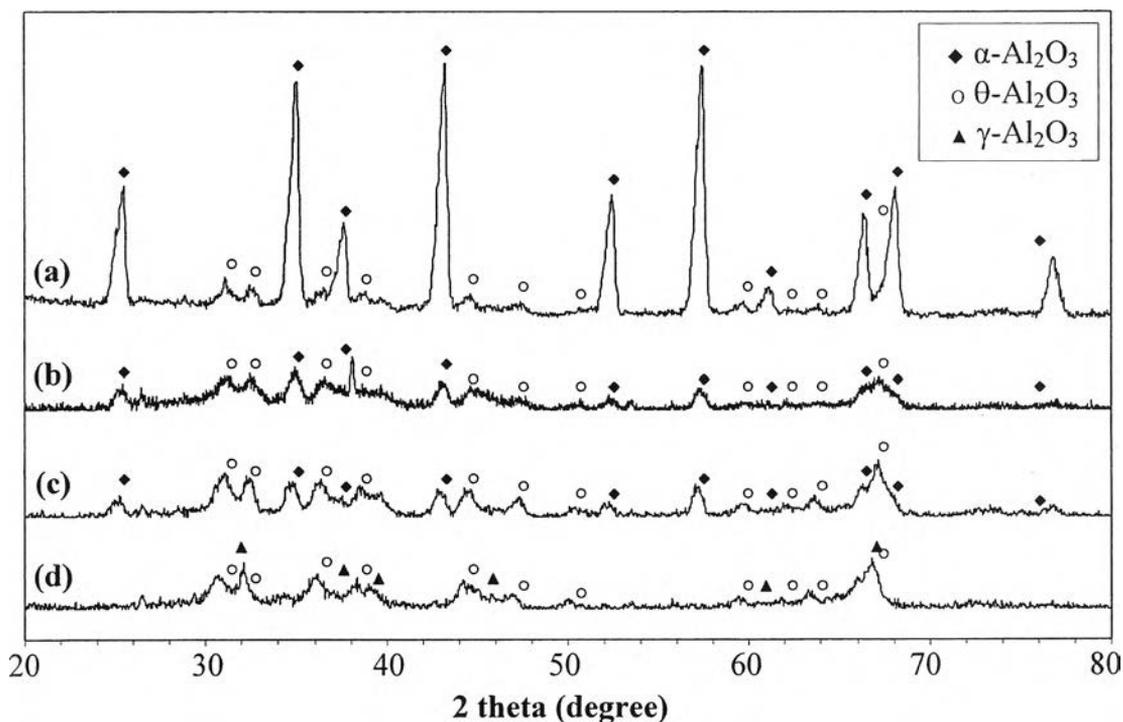
Figure 4.21 XRD patterns of electrospun nanofibers prepared with acid-to-AIP molar ratio of 0.15:1, after calcined at 1,200°C (a) and 1,100°C (b) for 2 hrs and that of the powders prepared with acid-to-AIP molar ratio of 1.5:1, after calcined at 1,200°C (c) and 1,100°C (d) for 2 hrs.

The difference in phase transformation caused by acid content behavior is much more obvious in electrospun fibers, as shown in Figure 4.21. The results show that only the fibers prepared with low acid ratio and calcined at 1,200°C (Figure 4.21(a)) are mainly α-Al_2O_3. For other preparation conditions, all fibers are predominantly θ-Al_2O_3. XRD patterns in Figure 4.21(b) and (c) show that pattern corresponding to α-Al_2O_3 is much lower in intensity comparing to that in Figure 4.20(a). The phase transformation is seriously retarded in the sample shown in Figure 4.21(d), in which no α-Al_2O_3 is observed, but γ-Al_2O_3 is still presented in the fibers even after calcined at 1,100°C.

According to the aforementioned results the transition temperature of alumina is influenced by amount of acid added during the sol-gel process. This retarding effect is more prominent in the electrospun nanofibers.

The structured of the calcined Al_2O_3 nanofibers prepared by various calcination temperatures and acid-to-AIP molar ratios were also studied by TEM (Figure 4.22 to 4.25). In Figure 4.22(a) and 4.23(a), fibers were produced from the solution with acid-to-AIP molar ratio of 0.15 and calcined under the calcination temperature of 1,100 and 1,200°C, respectively. The structure of the calcined fibers is changed from the aggregates of small grains to one large grain as the calcination temperature is increased. It is consistent with the results from XRD analysis shown in Figure 4.21, which indicate the major phase transformation from θ-Al_2O_3 to α-Al_2O_3 within the range of temperature investigated. SAED patterns in, Figure 4.22(b) also and 4.23(b) show that crystallinity of the fibers changes significantly when the calcination temperature is increased. This result has been discussed in details earlier in Section 4.2.

For comparison, the fibers prepared from the solution with acid-to-AIP molar ratio of 1.5 were also investigated by TEM (Figure 4.24 and 4.25). In general, grain size of the fibers is clearly increased with the increase in the calcination temperature, as shown in Figure 4.24(a) and 4.25(a). The spots of in the SAED images in Figure 4.24(b) and 4.25(b) illuminate more clearly, which indicates the increase in crystallinity of the fibers, as the calcination temperature is increased from 1,100 to 1,200°C.

It should also be noted that no large grain is observed in fibers with high acid ratio, even though the fibers were calcined at 1,200°C. This result relates to XRD results previously discussed, which shows θ-Al_2O_3 to be the major phase in the fibers prepared with high acid content instead of α-Al_2O_3. Thus, large-grain fibers observed in TEM are fibers in α-Al_2O_3 phase, while the aggregated-grains fibers are mainly θ-Al_2O_3 phase with initially formed α-Al_2O_3 phase.

(a)   (b)
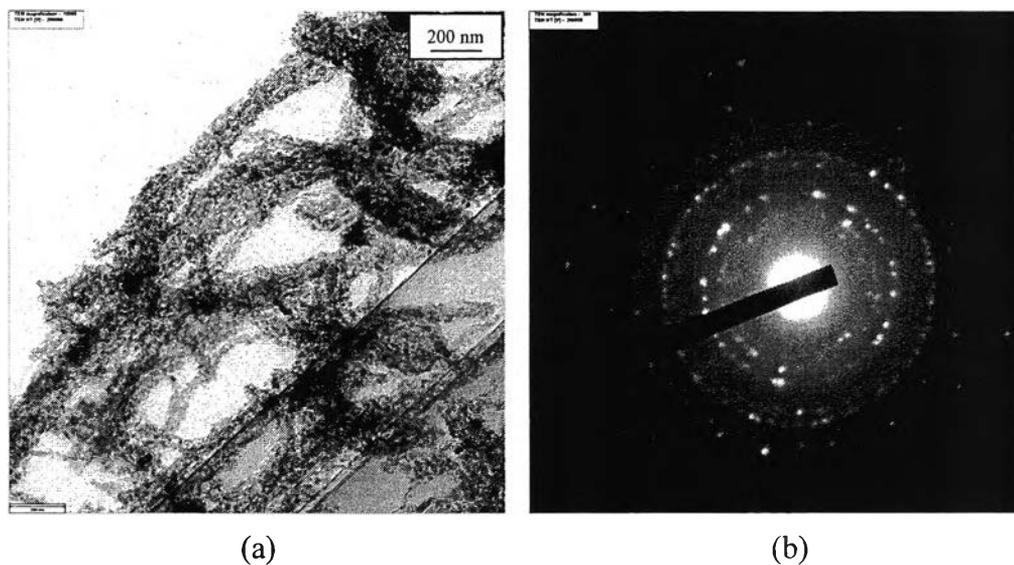
Figure 4.22 TEM micrograph of the composite fibers prepared with acid-to-AIP
molar ratio of 0.15:1 and calcined at 1,100°C for 2 hrs: (a) TEM image
and (b) SAED pattern.

(a)   (b)
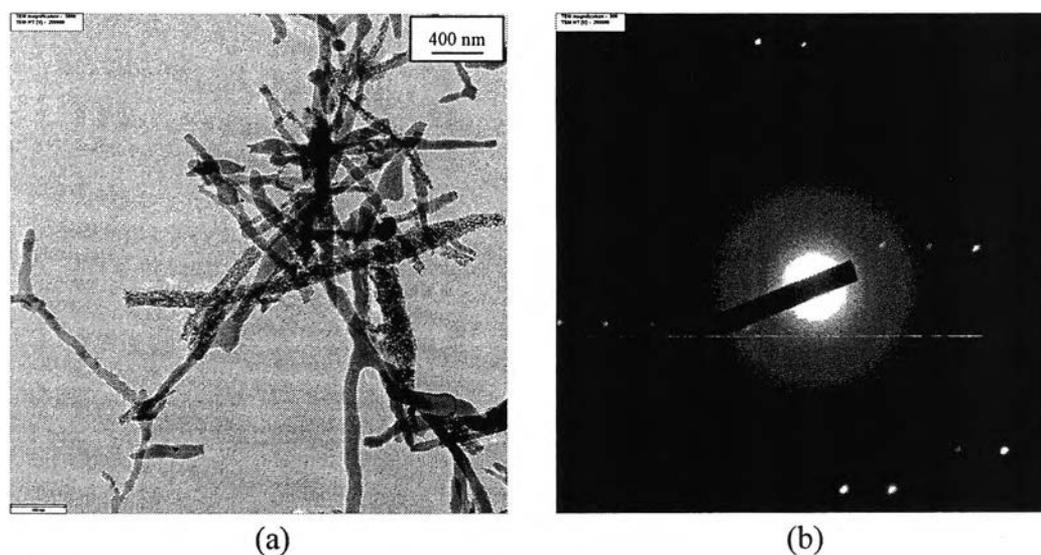
Figure 4.23 TEM micrograph of the composite fibers prepared with acid-to-AIP
molar ratio of 0.15:1 and calcined at 1,200°C for 2 hrs: (a) TEM image
and (b) SAED pattern.

<center>(a)   (b)</center>
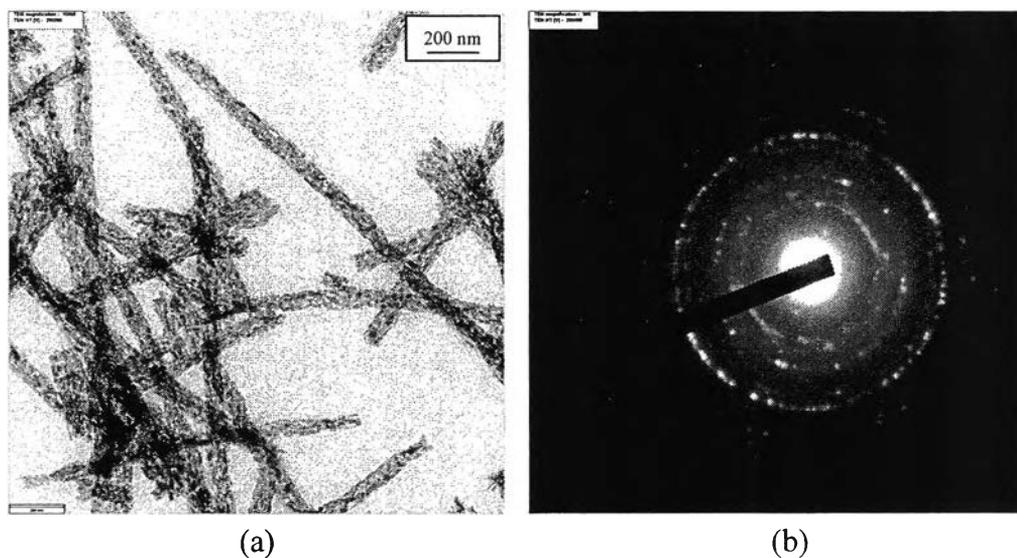
Figure 4.24 TEM micrograph of the composite fibers prepared with acid-to-AIP molar ratio of 1.5:1 and calcined at 1,100°C for 2 hrs: (a) TEM image and (b) SAED pattern.

<center>(a)   (b)</center>
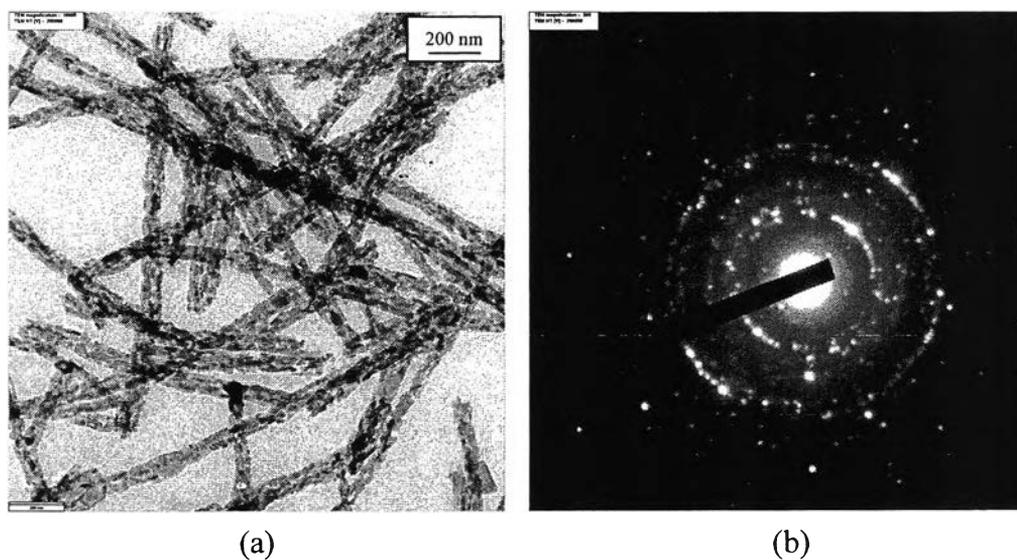
Figure 4.25 TEM micrograph of the composite fibers prepared with acid-to-AIP molar ratio of 1.5:1 and calcined at 1,200°C for 2 hrs: (a) TEM image and (b) SAED pattern.

FTIR characterization results of boehmite powders prepared with acid-to-AIP molar ratio of 0.15:1 and 1.5:1 are presented in Figure 4.26. The absorption band around 3,300 cm^{-1} arises from stretching mode of hydroxyl groups that involve in hydrogen bonding, as well as bridged hydroxyl groups [Teoh et al. 2007]. The appearance of a shoulder at wavenumber around 3,100 cm^{-1} ascertains the presence of pseudoboehmite phase, which is in agreement with XRD results. The bands at 1,630 and 1,615 cm^{-1} for the sample with acid-to-AIP ratio of 0.15:1 and 1.5:1 are corresponding to the bending vibration of weakly bound molecular water. The bands observed between 1,560 and 1,346 cm^{-1} in the samples could be the results from the presence of carbon-oxygen (C=O), carbon-carbon (C-C) and carbon-hydrogen (CH$_3$) deformation. For these as-prepared samples, the sharp absorption band around 1,070 cm^{-1} could be attributed to the bending mode of hydroxyl groups in alcohol, water and Al-OH-Al bonding. The shoulder at 1,150 cm^{-1} also corresponds to stretching mode of Al-OH-Al groups [Teoh et al. 2007]. Absorption in the region from 600 to 800 cm^{-1} arises from stretching modes of AlO$_4$ and AlO$_6$ as well as the vibrations of OH groups. The bending vibrations of AlO$_4$ are observed at 739 cm^{-1}, whereas the vibrations due to the bending modes of AlO$_6$ units occur at 642, 511 and 484 cm^{-1} [Teoh et al. 2007].

Boehmite, which has orthorhombic dipyramidal unit cell, has crystalline structure built up from layers of corner-sharing octahedrals [Wang et al. 1999]. The octahedrals are nearly undistorted and have four of their corners occupied by oxygen atoms and the other two by hydroxyls. According to Figure 4.26 by increasing the acid ratio, the definition in the Al-O stretching and bending vibrations at 742 and 644 cm^{-1} is gradually lost while the intensity of the Al-OH-Al bending vibrations at around 1070 cm^{-1} is increased. The results from FTIR analysis could be described by the previously report on the synthesis method for boehmite via sol-gel process, which consists of hydrolysis and condensation [Yoldas 1975]. As reported by Teoh et al. [Teoh et al. 2007], under acidic conditions, hydrolysis is favored and condensation is the rate-determining step. Therefore, a great number of small-hydroxylated oligomers with reactive Al-OH groups are simultaneously formed and thus fewer sites are available for condensation. For this reason, the results in both the sol and the gel under acidic condition are very uniform when compared with basic and neutral conditions [Gonzalez et al. 1997; Sharma et al. 2003].
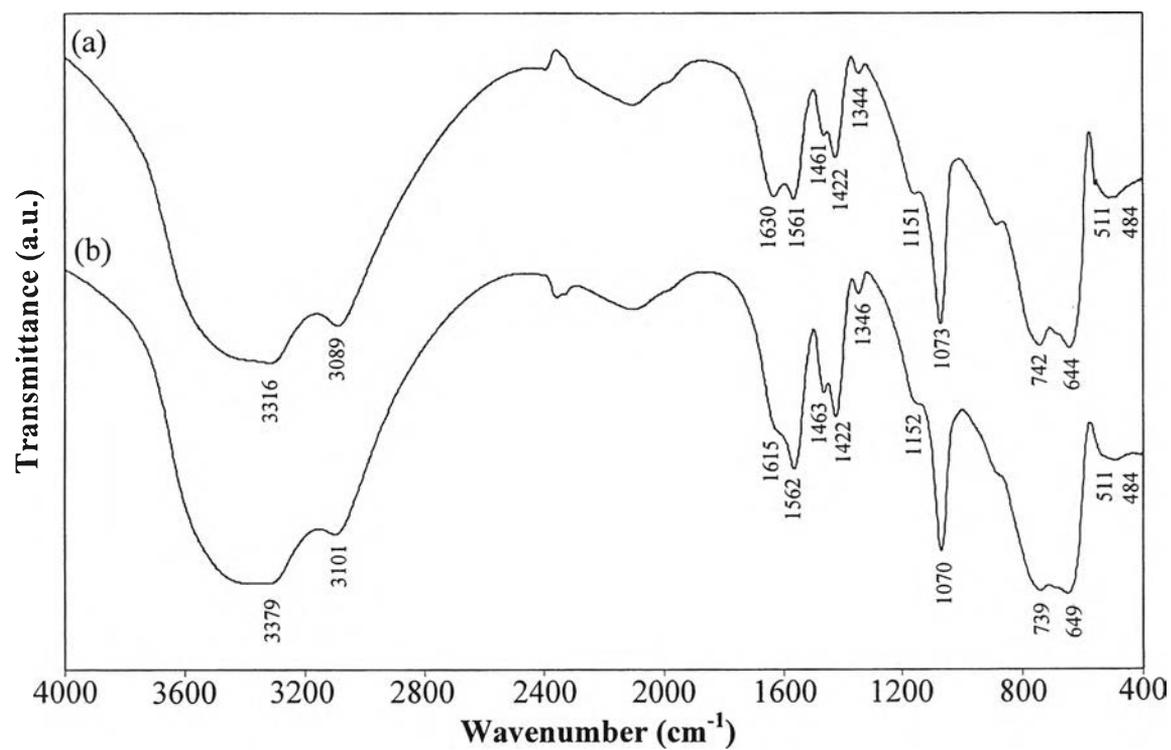
Figure 4.26 Normalized FTIR spectra of boehmite powders prepared with acid-to-AIP molar ratio of: (a) 0.15:1 and (b) 1.5:1.

The transformation of the AlOOH into an oxide produces FTIR absorption bands in the range between 640 and 840 cm⁻¹ (Figure 4.27). The broadening of the bands affirms the conversion from AlOOH to Al_2O_3. Moreover, the retarded phase transformation is clearly observed when the absorption bands between 707 and 834 cm⁻¹ are replaced by broad band at 759 cm⁻¹. These findings correspond with the results from XRD analysis, which have been described in the previous section.
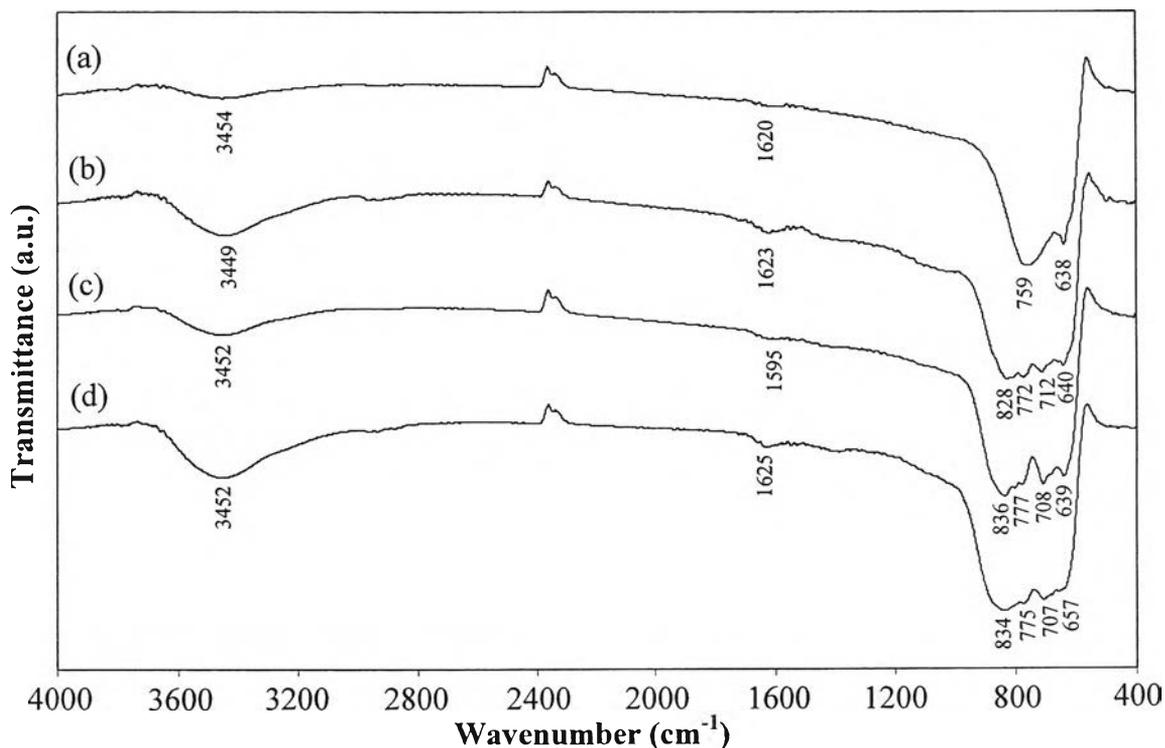
Figure 4.27 Normalized FTIR spectra of the fibers prepared with acid-to-AIP molar ratio of 0.15:1, after calcined at 1,200°C (a) and 1,100°C (b) for 2 hrs and that of the fibers prepared with acid-to-AIP molar ratio of 1.5:1, after calcined at 1,200°C (c) and 1,100°C (d) for 2 hrs.